

## Original Article

# Cytopathy of an infiltrating monocyte lineage during the early phase of infection with murine coronavirus in the brain

Hanae Takatsuki,<sup>1,2</sup> Fumihiro Taguchi,<sup>3,4</sup> Risa Nomura,<sup>1</sup> Hiromi Kashiwazaki,<sup>1</sup> Mariko Watanabe,<sup>5</sup> Yuzuru Ikehara<sup>6</sup> and Rihito Watanabe<sup>1</sup>

<sup>1</sup>Department of Bioinformatics, Faculty of Engineering, Soka University, Hachioji, Tokyo, <sup>2</sup>Laboratory of Molecular Biology of Infectious Agents, Graduate School of Biomedical Sciences, Nagasaki University, Nagasaki, <sup>3</sup>Laboratory of Respiratory Viral Diseases, National Institute of Infectious Diseases, Tokyo, <sup>4</sup>Nippon Veterinary and Life Science University, Musashino, Tokyo, <sup>5</sup>Department of Applied Biological Science, Tokyo University of Agriculture and Technology, Tokyo, and <sup>6</sup>Research Center for Medical Glycoscience, Ibaraki, Japan

**Viral spread during the early stages after infection was compared between a highly neurovirulent mouse hepatitis virus (MHV), JHMV cl-2 strain (cl-2), and its low-virulent mutant, soluble-receptor-resistant (srr)7. The infection of cells with srr7 (soluble-receptor-resistant mutant 7) is dependent on a known MHV receptor (MHVR), carcino-embryonic cell adhesion molecule 1a, whereas cl-2 shows MHVR-independent infection. Initial viral antigens were detected between 12 and 24 h post-inoculation (p.i) in the infiltrating cells that appeared in the subarachnoidal space of mouse brains infected with viruses. There were no significant differences in the intensity or spread of viral antigens in the inflammatory cells between the two viruses. However, 48 h after infection with cl-2, viral antigen-positive cells in the grey matter with the shape of neurons, which do not express MHVR, were detected, while srr7 infection was observed primarily in the white matter. Some of the viral antigen-positive inflammatory cells found in the subarachnoidal space during the early phase of infection reacted with anti-F4/80 or anti-CD11b monoclonal antibodies. Syncytial giant cells (SGCs) expressing viral and CD11b antigens were also detected among these inflammatory cells. These antigen-positive cells appeared in the subarachnoidal space prior to viral antigen spread into the brain parenchyma, indicating that viral encephalitis starts with the infection of infiltrating monocytes which express MHVR. Furthermore, the observation indicates**

**that viral infection has cytopathic effects on the monocyte lineage, which plays a critical role in innate immunity, leading to the rapid spread of viruses during the early stage of infection.**

**Key words:** CD11b, JHM, meningitis, neuropathology, syncytium.

## INTRODUCTION

Mouse hepatitis virus (MHV), a member of the coronavirus family, is an enveloped virus with single-stranded, positive-sense genomic RNA that is about 30 kilobases long.<sup>1</sup> Spike (S) protein, composed of virion projections, is responsible for binding to a receptor and also for the cell entry mechanism of MHV. The cell entry mechanism of MHV is thought to be similar to that of human immunodeficiency virus or other enveloped viruses.<sup>2</sup> Four different splice variants of MHV receptor (MHVR) are known to exist. They have either two or four ectodomains with long or short cytoplasmic tails.<sup>3,4</sup> Two allelic forms have been reported: one is CEACAM1a, which is expressed in most laboratory mouse strains, and the other is CEACAM1b, which is known thus far to be expressed by only the SJL mouse strain.<sup>5,6</sup> Although neurovirulent MHV strain JHMV induces encephalomyelitis by infecting a wide spectrum of brain cells including neurons,<sup>7–9</sup> MHVR has not been reported to exist within this wide range of infected cells in the CNS<sup>10</sup> except for microglia.<sup>11</sup> However, *in vivo* and *in vitro* experiments have shown that the infection of glial progenitors, oligodendrocytes and astrocytes, was blocked by pretreatment with the anti-MHVR antibody MAb CC1 or Ab-655,<sup>12</sup> which suggested that MHVR is

Correspondence: Rihito Watanabe, MD, Department of Bioinformatics, Faculty of Engineering, Soka University, 1-236 Tangi-chou, Hachioji, Tokyo 192-8577, Japan. Email: rihitow@soka.ac.jp

Received 30 July 2009; revised and accepted 15 October 2009; published online 28 December 2009.

essential for the initiation of MHV infection in the brain. In mixed neural cell cultures, cl-2 induced syncytia in most of the cells including neurons.<sup>11</sup> On the other hand, soluble-receptor-resistant (srr)7, which infects and spreads solely in an MHVR-dependent fashion,<sup>13</sup> infected a limited number of microglia marker-positive cells and infection did not spread, indicating that microglial cells are the initial target for MHV infection and that the wt spreads from initially infected microglia to a variety of cells in an MHVR-independent fashion, which suggested that MHVR is essential for the initiation of MHV infection in the brain. srr7 was isolated as an srr mutant, that is, the mutant virus is not neutralized with the soluble form of MHV receptor proteins. In general, the soluble receptor neutralizes virus infectivity.<sup>14-17</sup> This neutralization may be due to the ability of the soluble receptor to compete with the membrane-anchored receptor for virus binding.<sup>18</sup> Alternatively, the neutralization could be due to receptor-induced conformational changes of the envelope protein, which can no longer bind to the membrane-anchored receptor.<sup>13</sup> Although srr7 surface proteins show binding activity through the S1 region, an N-terminal subunit of the S protein, to the viral receptor, similar to that of wild-type cl-2 protein, srr7 is less virulent than cl-2. The reduced virulence and infectivity of srr7 compared with those of cl-2 could be attributed to the mutation of a single amino acid at position 1114 (Leu to Phe) in the S2 subunit of the viral surface protein,<sup>19</sup> which is not involved in receptor binding activity. This substitution in the S2 subunit could have brought about a structure less vulnerable to conformational changes in the S glycoprotein of srr7 virus compared to that of cl-2,<sup>18</sup> and causes reduced infectivity which occurs only in a receptor-dependent manner, leading to the reduced neurovirulence of srr7 compared to that of the wild-type, cl-2 virus.<sup>13</sup> The conformational changes in the S glycoprotein occur after binding of S1 to the receptor protein to induce fusogenic activities of the membrane-anchored fusion subunit, S2.<sup>20</sup>

This paper focused on viral spread during the initial phase of infection, especially at 24 h post-inoculation (p.i.), to determine the events that facilitate the dense exposure of the viruses to the cell surfaces of receptor-negative cells including neurons, providing an opportunity for receptor-independent infection in the micro-environments of the brain.

## METHODS

### Animals and viruses

Specific pathogen-free inbred BALB/c mice purchased from Charles River (Tokyo, Japan) were maintained according to the guidelines set by the committee of our

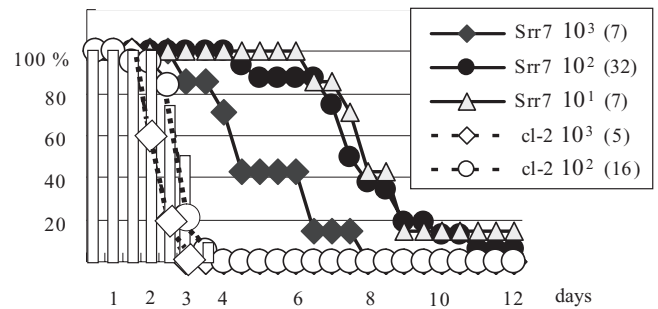


**Fig. 1** Survival of BALB/c mice following intra-cerebral inoculation with srr7 or cl-2 viruses at different doses ( $1 \times 10^1$ – $1 \times 10^3$  PFU). The figures in parentheses indicate the number of mice infected. White bars represent the survival rate of 12 ICR mice infected with  $10^2$  PFU of cl-2.

university. At 5 weeks old, 21 and 46 mice were inoculated with  $1 \times 10^1$ – $10^3$  of JHMV cl-2 or srr7 virus,<sup>21</sup> respectively, as indicated in Figure 1, into the right frontal lobe under deep anesthesia. Infected mice were killed at intervals, and organs and peripheral blood were aseptically isolated from animals and stored at  $-80^\circ\text{C}$  until titration. These organs in PBS were homogenized with a glass homogenizer and centrifuged at 620 g for 15 min. The infectivity in the supernatants was measured by a plaque assay using DBT cells, as described previously.<sup>21</sup> DBT cells were grown in Dullbecco's modified minimal essential medium (DMEM; Nissui, Tokyo, Japan) supplemented with 5% fetal bovine serum (FBS; Japan Bioserum, Hiroshima, Japan) and cultured at  $37^\circ\text{C}$  in humid conditions and 5%  $\text{CO}_2$ .

### Tissue preparation for histology

Kinetic tests for histological studies were performed every 12 h until 48 h p.i. To determine the virulence of the viruses to BALB/c mice, part of the infected mice were monitored every day until 12 days p.i. After exsanguination of the infected animals under deep anesthesia, parts of the removed brain, liver, spleen, and peripheral blood were frozen for viral titration and preparing frozen sections, and the remaining portions were fixed in 4% paraformaldehyde buffered with 0.12 M phosphate (PFA) to obtain paraffin-embedded sections for histological staining with HE and for enzyme immunohistochemistry.<sup>22</sup> Some of the infected mice were perfused with PFA via cardiac route followed by 2% glutaraldehyde fixation to obtain epon-embedded samples for electron-microscopic (JEM-1200EXII, JEOL, Tokyo, Japan) observation, as described previously.<sup>23</sup>

### Immunostaining and neuropathology

Viral antigens were visualized in paraffin sections or frozen sections by immunohistochemistry or by immunofluorescence, respectively, using the rabbit polyclonal antibody,

SP-1, or mouse monoclonal antibody (MAb).<sup>11,21</sup> Rat anti-mouse F4/80 either unlabeled or biotin-conjugated (Serotec, Oxford, UK or eBioscience, San Diego, CA, US, respectively), rat anti-mouse CD11b biotin-conjugated (BD Pharmingen, San Diego, CA, US), CD3ε-Alex488 (Biolegend, San Diego, CA, US), and rat anti-mouse CD31 biotin-conjugated (BD Pharmingen) MAbs were used to detect the infected cell type. As a second or third application, biotinylated, Alexafluor 488, or Alexafluor 564-labeled goat anti-rabbit IgG, Alexafluor 488 or Alexafluor 564-labeled goat anti-mouse IgG, or avidin-Alexafluor 488, Alexafluor 564, or avidin-peroxidase conjugate (Molecular Probes, Eugene, OR, US) were used, as described previously.<sup>11,21</sup> Immunohistochemical analysis of paraffin sections was carried out as previously described.<sup>22</sup> Briefly, after deparaffinization, sections were incubated with 50% normal mixed serum (fetal calf, calf, pig and horse) diluted in PBS prior to the first antibody application to block non-specific antibody binding. After primary antibody incubation, the non-specific activity of endogenous peroxidase was blocked by incubating sections with 0.3% H<sub>2</sub>O<sub>2</sub> in methanol. Washes in PBS were carried out between each step. For the peroxidase reaction, 0.2 mg/mL 3,3'-diaminobenzidine tetrahydrochloride (DAB) (DOTIDE DAB, Wako, Osaka, Japan) in 0.1 M Tris buffer (pH 7.6) was used.

The frequency of viral antigen appearance in the submeningeal space and brain parenchyma was scored after immunohistochemical staining for MHV antigens in coronal sections obtained from paraffin-embedded brain tissues at the level of the frontal lobe, thalamus, and pons and cerebellum. The number of viral antigen-positive cells in the total area examined was counted to score the frequency in the submeningeal space, as follows: +, a few antigen-positive cells; ++, more than 20 antigen-positive cells; +++, more than 100 antigen-positive cells. The degree of antigen expression in brain parenchyma was scored as follows: +, a few antigen-positive cells in total area; ++, more than 10 antigen-positive cells in the field at 10 × magnification (field × 10); +++, more than three fields (× 10) that contain more than 10 antigen-positive glial cells; +++, fields with more than 10 antigen-positive glial cells that occupy more than 70% of the area. To score the appearance of syncytial giant cells (SGCs), after counting the number of SGCs in the total area, the following was adopted: +, a few SGCs; ++, more than 10 SGCs; +++, more than 20 SGCs.

## RESULTS

### Virulence and neuro-pathogenicity of the viruses to BALB/c mice

The right frontal lobes of BALB/c mice were inoculated with  $1 \times 10^3$ ,  $1 \times 10^2$ , and  $1 \times 10^1$  PFU of cl-2 or srr7, and

mortality and clinical signs were assessed daily for 12 days after infection. All mice inoculated with  $1 \times 10^3$  PFU of cl-2 or srr7 died within 10 days post-infection (p.i.), although a difference in the survival time was evident (Fig. 1), showing similar virulence on the infection of ICR mice (Fig. 1 and Matsuyama *et al.*<sup>21</sup>). When survival was compared at 3 days p.i., the survival rates in mice inoculated with  $1 \times 10^3$  PFU of srr7 or cl-2 were 8/9 and 0/5, respectively (*P*-value of srr7 vs. cl-2 infection  $< 10^{-4}$ ), and those with  $1 \times 10^2$  PFU infection with srr7 or cl-2 were 31/32 and 3/16 (*P*-value of srr7 vs. cl-2 infection  $< 10^{-16}$ ). Some mice infected with srr7 at the dose of  $1 \times 10^2$  or 10 PFU survived beyond the observation period (Fig. 1).

Neuropathological investigation at 12 h p.i. for mice either with cl-2 or srr7 infection revealed no apparent destruction of the brain parenchyma, which appeared after 24 h p.i. (Figs 3d–j, 5h–l) with inflammatory cell infiltration. After 48 h p.i., a different distribution (Fig. 3d–h) and intensity of cl-2- and srr7-induced lesions became apparent, that is, rapid and widespread destructive changes in the grey matter of the brain infected with cl-2, whereas srr7 infection induced lesions after a longer incubation period than cl-2, with predilection to the white matter.

Prior to these destructive changes observed in the brain parenchyma, inflammatory cell infiltration occurred in the meninx at 12 h p.i. with either cl-2 or srr7 infection (Fig. 3a–c). This meningitis spread not only on the side of the injection site (right frontal lobe) but also to the other side of the brain and to the level of the pons and cerebellum (Fig. 3d–h). This meningeal infiltration gradually gained in intensity over the course of infection (Table 1), and, at 24 h p.i., infected SGCs appeared (Figs 3i–j, 4) in the meninx among the inflammatory cells, also increasing in number and frequency during the time-course of infection (Table 1). The SGCs became visible in the lateral ventricle at 36 h p.i. (Fig. 3j). These SGCs were not seen in the brain parenchyma, not even among infiltrating cells around blood vessels in the parenchyma (Fig. 4d–l). The appearance of the SGCs as well as meningeal cell infiltration gradually decreased after 72 h p.i. (data not shown).

### Kinetics of viral antigen appearance during the early phase of infection

As early as at 12 h p.i., when the viral titers of the infected brains remained at undetectable levels (Fig. 2), the infiltrating cells bearing viral antigens appeared in the subarachnoidal space of brains infected with cl-2 or srr7 (Fig. 3a, c and Table 1). Subsequently, the ratio of viral antigen-positive cells as well as the intensity of inflammation in the meninx increased gradually (Table 1 and Fig. 5a–c). There were no significant differences in the intensity or spread of viral antigens in the inflammatory

cells between the two viruses (Table 1). Because microglia/monocyte lineage plays an important role in MHV viral spread in mixed brain culture,<sup>11</sup> the presence of viral antigen-bearing monocytes in the inflammatory cells was investigated. Double staining by immunofluorescence of

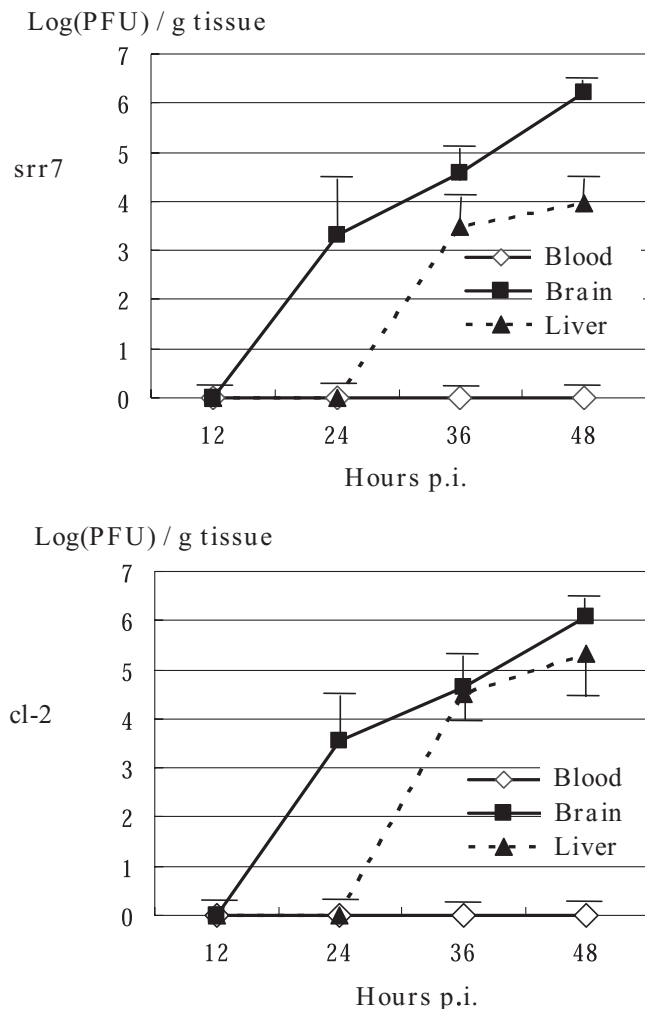


**Fig. 2** Viral growth during the early phase of infection in the peripheral blood, brain and liver. BALB/c mice were inoculated i.c. with  $1 \times 10^2$  PFU of srr7 or cl-2 virus. The organs were aseptically removed every 12 h after inoculation and virus titers in the homogenized tissues were plaque-assayed, as described previously.<sup>26</sup>

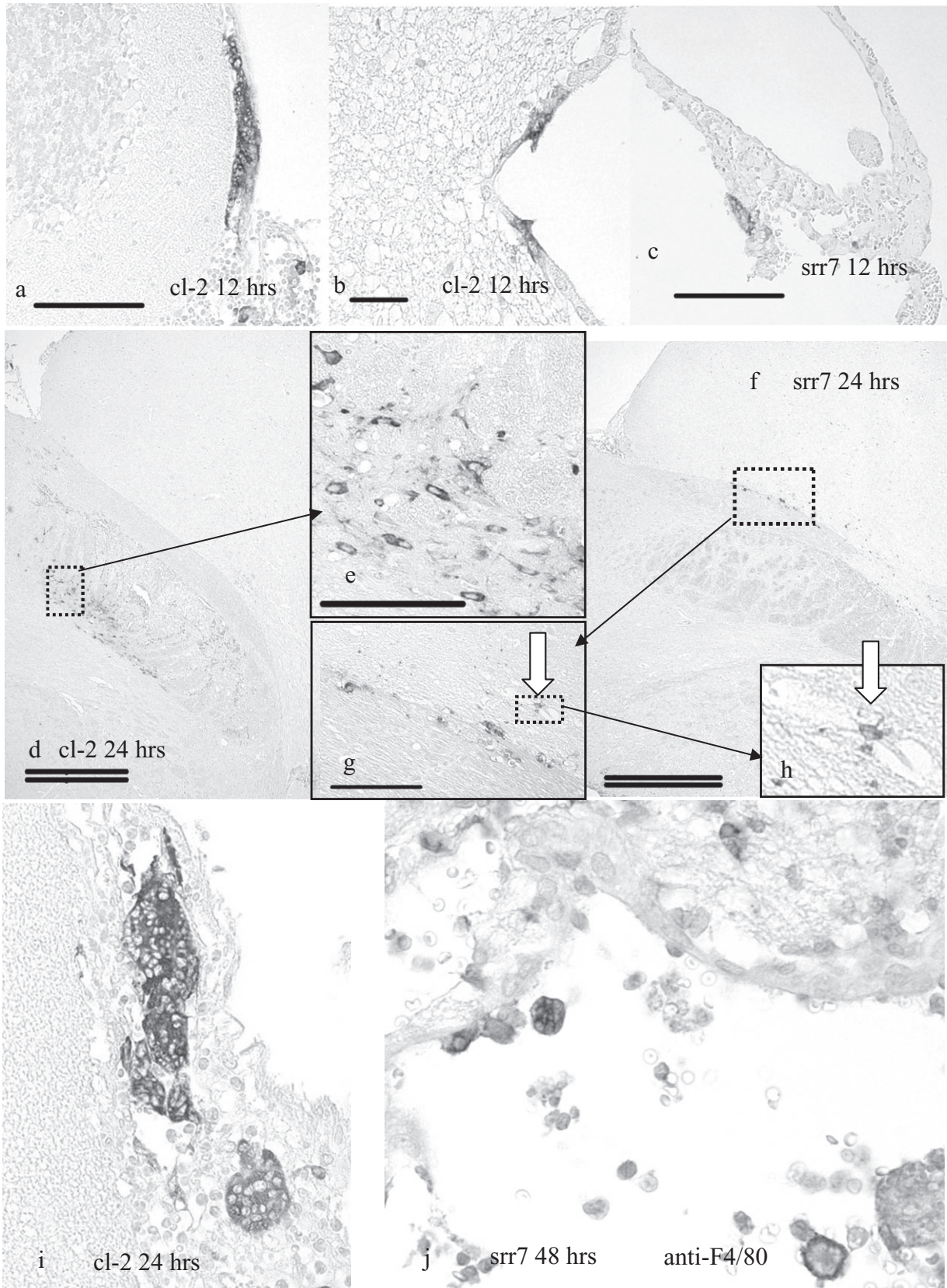
frozen sections revealed that some of the viral antigen-positive inflammatory cells found in the subarachnoid space during the early phase of infection reacted with anti-CD11b monoclonal antibodies (Fig. 5a–c). The viral antigen-positive monocytes accounted for approximately 10% of viral antigen-positive infiltrating cells seen in the subarachnoid space at 24 h p.i. (data not shown). All of the SGCs carried the viral antigens (Fig. 3i), and most of them expressed CD11b or F4/80 antigens (Fig. 3j). Besides these inflammatory cells, viral antigens during the early phase of infection were detected in the ependymal cells (Fig. 3b) and in the fibrous structures of the meninx (Fig. 3a) at 12 h p.i. Later, at 24 h p.i., viral antigen-positive fibrous structures were observed deep in the brain parenchyma (Fig. 5d–l). These viral antigen-positive structures might be correlated with the CD31-positive blood vessel architecture (long arrow in Fig. 5f) or unrelated (short arrows in Fig. 5d,f), and also be correlated with CD11b antigen (Fig. 5a–c,h–l) or unrelated (short arrows in Fig. 5a–c) as well. The viral antigen-positive cells in the brain parenchyma which became detectable at 24 h p.i. with cl-2 and srr7 infection showed a conspicuous difference in the distributions of the viral antigen spread between those induced by infections with these two viruses. In the brains infected with cl-2, viral antigens were

**Table 1** Appearance of viral antigens and syncytial giant cells (SGCs)

Virus	Hours post inoculation (a)	Meninx (b)	Brain	SGCs (d)
cl-2	12	±		
	24	++	+	+
	36	+++	++	++
	48	+++	+++	++
srr7	12	±	–	
	24	++	+	+
	36	++	++	++
	48	++	++	++

(a): Kinetic tests for histological studies were performed every 12 h until 48 h post inoculation (b, c): The frequency of viral antigen appearance in the submeningeal space (b) and brain parenchyma (c) was scored after immunohistochemical staining for mouse hepatitis virus antigens in coronal sections, as described in Materials and Methods. (d): After counting the number of SGCs in the total area, the degree was scored as described in Materials and Methods.

**Fig. 3** Immunostaining of paraffin sections for viral antigens (a–i) and F4/80 (j), prepared from mice at 12 (a–c), 24 (d–i) and 48 (j) hours post inoculation (p.i.). The infected viruses are indicated in each picture. At 12 h p.i., the viral antigens were already detected in the submeningeal space (a and c) and ependymal cells facing the 4th ventricle (b). At 24 h p.i., viral antigens spread into the brain parenchyma (d–h). cl-2-viral antigens appear in the grey matter of the basal ganglia where viral antigen-positive cells with the shape of neurons are detectable (d and e with a larger magnification of the dotted area in d), whereas srr7-infected cells are observed outside the basal ganglia (f and arrows in g and h); enlarged pictures of dotted areas (f and g) show fine projections of the cytoplasm typical of glial cell architecture. At the same time as viral infection into the brain parenchyma started, syncytial giant cells (SGCs) bearing viral antigens appeared in the submeningeal space (i). SGCs are also found in the ventricle (j). Many of the SGCs expressed F4/80 antigen (j). Single and double bars indicate 100 and 40  $\mu$ m, respectively.



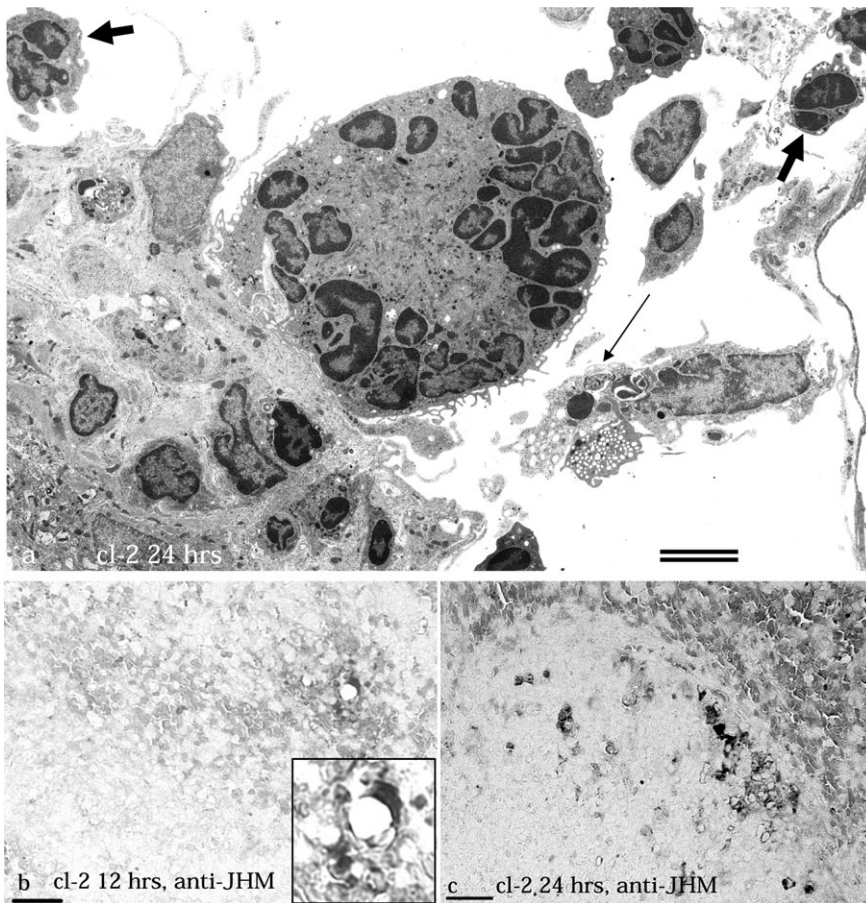


**Fig. 4** (a) An electron-microscope image of an syncytial giant cell (SGC) observed among other infiltrating cells including polynuclear leukocytes (arrows) in the submeningeal space of a cl-2-infected mouse at 24 h post inoculation (p.i.). Note the apoptotic cell (long arrow) with pycnosis. (b and c) Immunohistochemistry for the viral antigens in paraffin-embedded sections of the spleen at 12 and 24 h p.i., respectively. The sections are faintly stained with eosin to point out the area of erythrocyte-rich red pulp shown as a grey zone, clearly contrasting with the brighter area of the white pulp. At 12 h p.i., the viral antigens were detected mainly in the red pulp (b) with an enlarged picture of the squared area. At 24 h p.i., many viral antigen-positive cells appear in the white pulp (c). Double and single bars indicate 8 and 50  $\mu\text{m}$ , respectively.

already detectable in the grey matter in the initial phase of infection (Fig. 3d–e), whereas in brains infected with srr7, MHV viral antigens were detected mainly in the white matter (Fig. 3f–h), showing close agreement with our previous report.<sup>21</sup> However, until now, attempts at the specific characterization of these viral antigen-positive cells in the white matter have not been successful using anti-basic protein for oligodendrocytes or GFAP for astrocytes (data not shown). Only a few of the viral antigen-positive glial cells detected after infection with srr7 carried the CD11b antigen together with viral antigens (Fig. 5h–l).

A possibility that the infection of these inflammatory cells is caused by preceding viremia was considered to be unlikely, because antigen-positive cell infiltration in the subarachnoid space was already observed at 12 h p.i. Furthermore, virus in the peripheral blood was not detected at 24 h p.i. (Fig. 2). In order to assess this, we checked the viral spread in the spleen. Surprisingly, at 12 h p.i., viral antigen-positive cells were detected in the red pulp of the spleen (Fig. 4b). As in the brain, the viral antigen-positive cells were increased in number and they were deeply distributed in the white pulp at 24 h p.i. (Fig. 4c). Interestingly, both in the brain and spleen, the initial viral antigens were detected along with the blood

flow, in the meningeal spaces of the brain and red pulp of the spleen at 12 h p.i., and after 24 h p.i. the locations of viral antigen presence extended to the deeper region of the tissues as if they were guided by the infected blood vessel walls to the brain parenchyma or the T-cell zone in the white pulp of the spleen (Fig. 5m). The viral antigen-positive architecture of a blood vessel was found to enter the T-cell zone, visualized in Fig. 5m as a CD3 $\epsilon$ -positive cell area.

## DISCUSSION

There were no distinct differences in the susceptibilities of the two mice strains, BALB/c and ICR mice, either to cl-2 or srr7, although there was a slightly shorter incubation period in BALB/c mice (Fig. 1) than in ICR mice.<sup>21</sup> In addition, neither neuropathological changes nor the MHV viral antigen distribution caused by cl-2 or by srr7 infection showed fundamental differences between BALB/c (Figs 3,4) and ICR mice.<sup>21</sup> The neuropathological changes induced by cl-2 or srr7 infection into BALB/c mice after 48 h p.i. were the same, with the exception of a description of the appearance of infected SGCs, as already described in a previous report<sup>21</sup> using ICR mice.

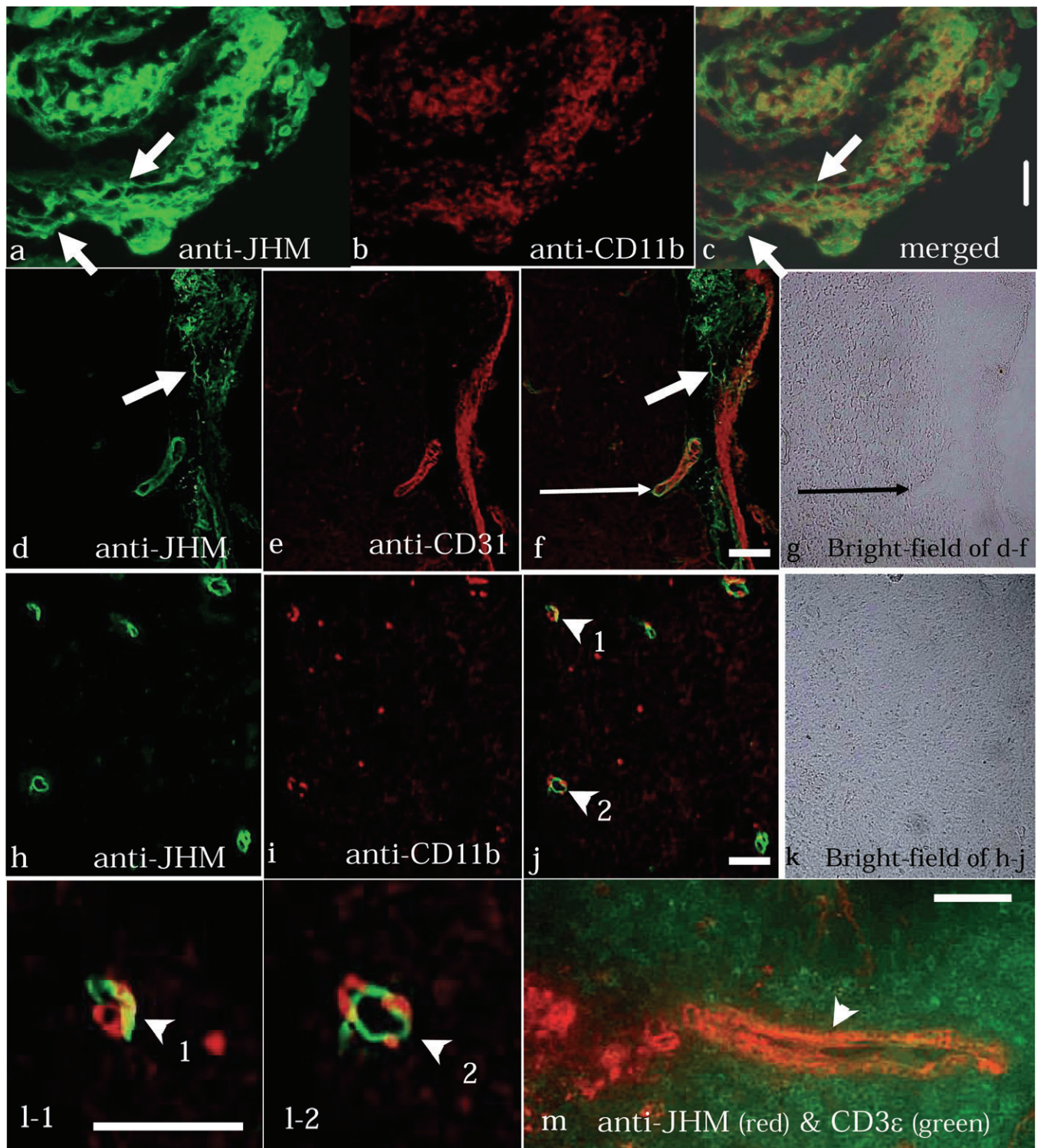


**Fig. 5** Immunofluorescent pictures on frozen sections. Antibodies used are illustrated in each picture. (a–c) Submeningeal inflammatory cells carrying viral antigens (a) at the level of left cerebellum at 24 h post inoculation (p.i.) with cl-2. Many CD11b-positive cells are infected (b–c). (d–g) 24 h p.i. with srr7. An architecture of blood vessels positive for both CD31 (e, f) and viral antigens (d, f) extends into the brain cortex (long arrows in f and g). Note the fibrous structures positive for viral antigens (bold arrows) unrelated to the CD11b-positive cells (a–c) or architecture of blood vessels (d–f). (h–l) Thalamus at 24 h p.i. with cl-2. Many architectures of small blood vessels are infected (h), and associated with CD11b positive cells (i–j, l-1 and l-2). Only few overlaps of viral antigens and CD11b are observed. l-1 and l-2 illustrate a higher magnification of the numbered area in j. (m) Spleen at 24 h p.i. double-stained for viral antigens (red) and T-cells (green). The cellular components carrying viral antigens and unrelated to the architecture of the blood vessel (arrow head) are mainly located in the dark area (outside the T-cell zone). The vertical and horizontal bars indicate 50 and 25  $\mu$ m, respectively.

Initial viral antigens were detected at 12 h p.i. in the infiltrating cells that appeared in the subarachnoidal space of mouse brains infected with the viruses. There were no significant differences in the intensity or spread of viral antigens in the inflammatory cells between the two viruses (Table 1). However, 24 h after infection with cl-2, viral antigen-positive cells in the grey matter with the shape of neurons were detected (Fig. 3d,e). Neurons do not reportedly express MHVR.<sup>10–12</sup> In contrast, viral antigen-positive cells after infection with srr7 were mainly distributed in the white matter (Fig. 3f–h). Some of the viral antigen-positive inflammatory cells found in the subarachnoidal space during the early phase of infection reacted with anti-F4/80 or anti-CD11b antibodies (Figs 3j,5a–c). These antigen-positive cells appeared in the subarachnoidal space prior to viral spread into the brain parenchyma, indicating that viral encephalitis starts with infection of the infiltrating monocyte lineage which expresses MHVR,<sup>24</sup> and that viremia contributes to the spread of the viruses. However, at 12 h p.i., the viral titers obtained from brains or peripheral blood of the mice infected either with cl-2 or srr7 remained at undetectable levels (Fig. 2). It is not clear where these infiltrating cells were infected. They might be infected at the site of inoculation after inflammation due to mechanical injury caused by the needle for virus injection. Blood vessels can be a source of secondary infection for infiltrated cells because endothelial cells express MHVR,<sup>12</sup> but it is too short a time for them to undergo secondary infection at 12 h p.i.<sup>25</sup> Another possibility is that circulating viruses in the peripheral blood below detectable levels could reach lymphoid organs, from where the infected cells might well target the inflammatory site in the subarachnoidal space. Actually, infected cells were detected in the red pulp of the spleen at 12 h p.i. (Fig. 4b). The abrupt extension of viral antigen localization deep into the T-cell zone in the spleen after 24 h p.i. (Fig. 5m) might be mediated by a conduit system reaching to the splenic white pulp,<sup>26</sup> including to T-cell zones.<sup>27</sup> Although endothelial cells express the MHV receptor and MHV can bind to endothelial cells via this receptor,<sup>28</sup> further careful examination is required to determine whether it is the infected endothelial cells that guide the extension of the infection into the parenchyma, perivascular fibrous apparatus comprising a conduit system, or if monocyte lineages play an important role. Infiltrated monocytes which stick to the blood vessels are often indistinguishable from endothelial cells on light microscopic observation.<sup>29</sup>

Among the infiltrating cells in the subarachnoidal space, SGCs were found during the early phase of infection (Fig. 3i). All of the SGCs bore the viral antigens (Fig. 3i). The SGCs appeared during the early phase of infection almost at the same ratio and with the same distribution in animals infected either with srr7 and cl-2 (Table 1). Conse-

quently, it might be concluded that these SGCs do not contribute to the different neuro-pathogeneses induced by infection with srr7 and cl-2. However, the appearance of syncytium formation in circulating leukocytes indicates that the viruses are able to induce direct cytopathic effects on the infected immuno-competent cells, leading to a rapid spread of the viruses during a very early phase of infection, overcoming the innate immunity of hosts, which is induced at the earliest step of viral infection through the recognition of viral components by host pattern-recognition receptors such as the Toll-like receptor family.<sup>30,31</sup> Interferon (IFN) receptor expression in monocyte lineage or dendritic cells can play a primary role in the early containment of MHV,<sup>32</sup> in addition to the role of INF production in infected tissue.<sup>33</sup> In the case of cl-2 infection, the rapid viral spread which can be accelerated by receptor-independent infection of the virus,<sup>25</sup> possibly infecting receptor-unexpressed neurons in the grey matter as early as 24 h p.i. (Fig. 3d,e), could bring about the death of infected mice in a very short time after viral inoculation within 2–3 days p.i. (Fig. 1). During this time, the host's adaptive immune reaction against the virus has yet to be initiated,<sup>10,34</sup> which mediates protection from lethal coronavirus encephalomyelitis caused by other JHM strains of MHV<sup>35</sup> after propagating a successful innate immune response, owing much to type I interferon production.<sup>36</sup> In contrast, infection with srr7, which spreads in a receptor (CEACAM1a)-dependent manner,<sup>25</sup> does not induce such a rapid death of infected mice (Fig. 1 and Matsuyama *et al.*<sup>21</sup>), in the absence of infecting critical targets, such as neurons, in the CNS. Nevertheless, srr7, which differs only in one amino acid sequence in the S region,<sup>13</sup> successfully propagates in the CNS, shown by the compatible viral growth compared with cl-2 determined by a titration assay (Fig. 2). Therefore, srr7 as well as cl-2 infection could have induced a rapid viral spread in the infected CNS after effectively suppressing initial innate immunity through inducing cytopathic effects on the infected immuno-competent infiltrating cells during the initial phase of infection, probably in addition to the effects of the nucleocapsid gene expression on the down regulation of type I interferon production, which alone seems to be insufficient to suppress such a rapid spread of the viruses after infection with cl-2 or srr7 reaching the spleen within 12 h p.i. intra-cerebrally.

The cytopathic effects of the viruses observed as SGCs among infiltrating cells could have been induced by the infection of infiltrated monocyte lineages including phagocytes, because many of these SGCs carried the F4/80 antigen (Fig. 3j) as well as viral antigens (Fig. 3i). In some SGCs, monocyte-marker antigens, such as F4/80, CD11b, or CD68, were not detected by immuno-labeling methods (data not shown). The failure of F4/80-expression in some

SGCs could be due to the down-regulation of the antigens. Many cytopathic RNA viruses, such as paramyxovirus,<sup>37</sup> vesicular stomatitis virus, poliovirus, and influenza virus, as well as MHV, inhibit the translation of host mRNAs while selectively translating viral mRNAs, and it is thought that this reduced host gene expression aids in the inhibition of antiviral responses.<sup>38</sup> None of the SGCs were labeled with antibodies for lymphoid cell antigens such as CD11c, B220, or CD3e (data not shown), indicating that the majority of SGCs are derived from infected monocyte lineages. Among the other infiltrating cells in the submeningeal space or cells in the spleen, many of the infected cells remained uncharacterized, after using antibodies for the characterization of SGCs described above. The limitation of the technique to identify cellular antigen expression after MHV infection by employing immuno-labeling methods *in vivo* is reportedly overcome by the *in vitro* or *ex vivo* analysis of CNS tissue culture<sup>11,12</sup> and splenic cells.<sup>39</sup> Further *ex vivo* and *in vitro* studies of infiltrating cells are ongoing in our laboratory.

The reason why SGCs became undetectable in the later phase of infection is unclear. One possibility is that MHVR (CEACAM1a) expression is down-regulated over the course of acute infection with JHM viruses and restored following immune-mediated virus control.<sup>10</sup> In addition to a blockage of the new infection of infiltrated monocytes due to the reduction of receptor expression, the host's immune response occurs during acute infection after 3 days p.i.,<sup>40</sup> through the contribution of CD8<sup>41</sup> and CD4<sup>42</sup> components, which may remove the infiltrated and infected cells in the submeningeal space, where immunosurveillant cells can reach more easily than the brain parenchyma, and, actually only a few infected cells are detectable 5 days after infection in the submeningeal space, although many viral antigens are detectable in the infected brain parenchyma at the same time.<sup>21</sup> The association of viral antigens with blood vessel walls in the brain also disappeared after 3 days p.i. (data not shown), which is consistent with a previous report that showed no detectable *in vivo* viral replication in endothelial cells from the brain at or after 3 days p.i. with MHV, in contrast to the equivalent cells from the liver where viral infection of endothelial cells was detected.<sup>28</sup> The extremely rapid spread and the shift of the viral antigen-distribution in the course of diseases induced by cl-2- and srr7-infection demonstrated in this paper are distinct from encephalomyelitis induced by other types of neuropathogenic MHVs appearing in previous reports, and might be a cause of high virulence observed in emergent viruses such as severe acute respiratory syndrome (SARS)-coronavirus<sup>43</sup> or mutated influenza viruses,<sup>44</sup> which could occur after suppressing initial innate immunity within 12 h p.i. Therefore, we propose the manner of the rapid spread of infection presented in this paper, that is, the rapid

viral spread from one organ or part of the initially infected site to another non-adjacent organ or part detected within 12 h after infection, to be designated as super-acute spread (SAS).

## ACKNOWLEDGEMENTS

This work was financially supported in part by grants from the Ministry of Education, Culture, Sports, Science and Technology.

## REFERENCES

1. Kubo H, Yamada YK, Taguchi F. Localization of neutralizing epitopes and the receptor-binding site within the amino-terminal 330 amino acids of the murine coronavirus spike protein. *J Virol* 1994; **68**: 5403–5410.
2. Sodroski JG. HIV-1 entry inhibitors in the side pocket. *Cell* 1999; **99**: 243–246.
3. Beauchemin N, Draber P, Dveksler G *et al.* Redefined nomenclature for members of the carcinoembryonic antigen family. *Exp Cell Res* 1999; **252**: 243–249.
4. Dveksler GS, Pensiero MN, Cardellichio CB *et al.* Cloning of the mouse hepatitis virus (MHV) receptor: expression in human and hamster cell lines confers susceptibility to MHV. *J Virol* 1991; **65**: 6881–6891.
5. Dveksler GS, Pensiero MN, Dieffenbach CW *et al.* Mouse hepatitis virus strain A59 and blocking antireceptor monoclonal antibody bind to the N-terminal domain of cellular receptor. *Proc Natl Acad Sci U S A* 1993; **90**: 1716–1720.
6. Yokomori K, Lai MM. The receptor for mouse hepatitis virus in the resistant mouse strain SJL is functional: implications for the requirement of a second factor for viral infection. *J Virol* 1992; **66**: 6931–6938.
7. Lavi E, Suzumura A, Hirayama M *et al.* Coronavirus mouse hepatitis virus (MHV)-A59 causes a persistent, productive infection in primary glial cell cultures. *Microb Pathog* 1987; **3**: 79–86.
8. Parra B, Hinton DR, Marten NW *et al.* IFN-gamma is required for viral clearance from central nervous system oligodendroglia. *J Immunol* 1999; **162**: 1641–1647.
9. Stohlman SA, Bergmann CC, van der Veen RC, Hinton DR. Mouse hepatitis virus-specific cytotoxic T lymphocytes protect from lethal infection without eliminating virus from the central nervous system. *J Virol* 1995; **69**: 684–694.
10. Ramakrishna C, Bergmann CC, Holmes KV, Stohlman SA. Expression of the mouse hepatitis virus receptor by central nervous system microglia. *J Virology* 2004; **78**: 7828–7832.

11. Nakagaki K, Taguchi F. Receptor-independent spread of a highly neurotropic murine coronavirus JHMV strain from initially infected microglial cells in mixed neural cultures. *J Virol* 2005; **79**: 6102–6110.
12. Godfraind C, Langreth SG, Cardellicchio CB *et al*. Tissue and cellular distribution of an adhesion molecule in the carcinoembryonic antigen family that serves as a receptor for mouse hepatitis virus. *Lab Invest* 1995; **73**: 615–627.
13. Taguchi F, Matsuyama S. Soluble receptor potentiates receptor-independent infection by murine coronavirus. *J Virology* 2002; **76**: 950–958.
14. Balliet JW, Berson J, D’Cruz CM *et al*. Production and characterization of a soluble, active form of Tva, the subgroup A avian sarcoma and leukosis virus receptor. *J Virol* 1999; **73**: 3054–3061.
15. Greve JM, Forte CP, Marlor CW *et al*. Mechanisms of receptor-mediated rhinovirus neutralization defined by two soluble forms of ICAM-1. *J Virol* 1991; **65**: 6015–6023.
16. Hussey RE, Richardson NE, Kowalski M *et al*. A soluble CD4 protein selectively inhibits HIV replication and syncytium formation. *Nature* 1988; **331**: 78–81.
17. Kaplan G, Freistadt MS, Racaniello VR. Neutralization of poliovirus by cell receptors expressed in insect cells. *J Virol* 1990; **64**: 4697–4702.
18. Matsuyama S, Taguchi F. Receptor-induced conformational changes of murine coronavirus spike protein. *J Virol* 2002; **76**: 11819–11826.
19. Saeki K, Ohtsuka N, Taguchi F. Identification of spike protein residues of murine coronavirus responsible for receptor-binding activity by use of soluble receptor-resistant mutants. *J Virol* 1997; **71**: 9024–9031.
20. Zelus BD, Schickli JH, Blau DM, Weiss SR, Holmes KV. Conformational changes in the spike glycoprotein of murine coronavirus are induced at 37 degrees C either by soluble murine CEACAM1 receptors or by pH 8. *J Virology* 2003; **77**: 830–840.
21. Matsuyama S, Watanabe R, Taguchi F. Neurovirulence in mice of soluble receptor-resistant (srr) mutants of mouse hepatitis virus: intensive apoptosis caused by less virulent srr mutant. *Arch Virol* 2001; **146**: 1643–1654.
22. Watanabe R, Takase-Yoden S. Neuropathology induced by infection with Friend murine leukemia viral clone A8-V depends upon the level of viral antigen expression. *Neuropathology* 2006; **26**: 188–195.
23. Takase-Yoden S, Watanabe R. Unique sequence and lesional tropism of a new variant of neuropathogenic friend murine leukemia virus. *Virology* 1997; **233**: 411–422.
24. Kammerer R, Stober D, Singer BB, Obrink B, Reimann J. Carcinoembryonic antigen-related cell adhesion molecule 1 on murine dendritic cells is a potent regulator of T cell stimulation. *J Immunol* 2001; **166**: 6537–6544.
25. Watanabe R, Matsuyama S, Taguchi F. Receptor-independent infection of murine coronavirus: analysis by spinoculation. *J Virol* 2006; **80**: 4901–4908.
26. Nolte MA, Belien JAM, Schadee-Eestermans I *et al*. A conduit system distributes chemokines and small blood-borne molecules through the splenic white pulp. *J Exp Medicine* 2003; **198**: 505–512.
27. Bajenoff M, Glaichenhaus N, Germain RN. Fibroblastic reticular cells guide T lymphocyte entry into and migration within the splenic T cell zone. *J Immunology* 2008; **181**: 3947–3954.
28. Godfraind C, Havaux N, Holmes KV, Coutelier JP. Role of virus receptor-bearing endothelial cells of the blood-brain barrier in preventing the spread of mouse hepatitis virus-A59 into the central nervous system. *J Neurovirol* 1997; **3**: 428–434.
29. Lassmann H, Zimprich F, Vass K, Hickey WF. Microglial cells are a component of the perivascular glia limitans. *J Neurosci Res* 1991; **28**: 236–243.
30. Kawai T, Akira S. Innate immune recognition of viral infection. *Nature Immunology* 2006; **7**: 131–137.
31. Garcia-Sastre A, Biron CA. Type 1 interferons and the virus-host relationship: a lesson in detente. *Science* 2006; **312**: 879–882.
32. Cervantes-Barragan L, Kalinke U, Zust R *et al*. Type I IFN-mediated protection of macrophages and dendritic cells secures control of murine coronavirus infection. *J Immunology* 2009; **182**: 1099–1106.
33. Malone KE, Stohlman SA, Ramakrishna C, Macklin W, Bergmann CC. Induction of class I antigen processing components in oligodendroglia and microglia during viral encephalomyelitis. *Glia* 2008; **56**: 426–435.
34. Gonzalez JM, Bergmann CC, Ramakrishna C *et al*. Inhibition of interferon-gamma signaling in oligodendroglia delays coronavirus clearance without altering demyelination. *American J Pathology* 2006; **168**: 796–804.
35. Savarin C, Bergmann CC, Hinton DR, Ransohoff RM, Stohlman SA. Memory CD4(+) T-Cell-Mediated Protection from Lethal Coronavirus Encephalomyelitis. *J Virology* 2008; **82**: 12432–12440.
36. Ireland DDC, Stohlman SA, Hinton DR, Atkinson R, Bergmann CC. Type I interferons are essential in controlling neurotropic coronavirus infection irrespective of functional CD8 T cells. *J Virology* 2008; **82**: 300–310.
37. Gainey MD, Dillon PJ, Clark KM, Manuse MJ, Parks GD. Paramyxovirus-induced shutoff of host and viral protein synthesis: role of the P and V proteins in limiting PKR activation. *J Virol* 2008; **82**: 828–839.

38. Lyles DS. Cytopathogenesis and inhibition of host gene expression by RNA viruses. *Microbiol Mol Biol Rev* 2000; **64**: 709–724.
39. Zhou HX, Perlman S. Preferential infection of mature dendritic cells by mouse hepatitis virus strain JHM. *J Virology* 2006; **80**: 2506–2514.
40. Iacono KT, Kazi L, Weiss SR. Both spike and background genes contribute to murine coronavirus neurovirulence. *J Virology* 2006; **80**: 6834–6843.
41. Bergmann CC, Parra B, Hinton DR, Ramakrishna C, Dowdell KC, Stohlman SA. Perforin and gamma interferon-mediated control of coronavirus central nervous system infection by CD8 T cells in the absence of CD4 T cells. *J Virology* 2004; **78**: 1739–1750.
42. Stohlman SA, Hinton DR, Parra B, Atkinson R, Bergmann CC. CD4 T cells contribute to virus control and pathology following central nervous system infection with neurotropic mouse hepatitis virus. *J Virology* 2008; **82**: 2130–2139.
43. Matsuyama S, Ujike M, Morikawa S, Tashiro M, Taguchi F. Protease-mediated enhancement of severe acute respiratory syndrome coronavirus infection. *Proc Natl Acad Sci United States America* 2005; **102**: 12543–12547.
44. Neumann G, Noda T, Kawaoka Y. Emergence and pandemic potential of swine-origin H1N1 influenza virus. *Nature* 2009; **459**: 931–939.